Simultaneous Demand Response Program and Conservation Voltage Reduction for Optimal Operation of Distribution Systems

Conference Paper · October 2020

DOI: 10.1109/IAS44978.2020.9334720

5 authors, including:

Tohid Khalili
University of New Mexico

Amirreza Jafari
University of Tabriz

Behnam Mohammadi-ivatloo
University of Tabriz

Ali Bidram
University of New Mexico

Simultaneous Demand Response Program and Conservation Voltage Reduction for Optimal Operation of Distribution Systems

Tohid Khalili, *Student Member, IEEE*, Amirreza Jafari, Seyed Mohammad Sajjadi Kalajahi, Behnam Mohammadi-Ivatloo, *Senior Member, IEEE,* Ali Bidram*, Senior Member, IEEE*

***Abstract*—Electric loads' power consumption depends on their terminal voltage. Therefore, one can slightly change the active and reactive power of loads by changing their terminal voltage. Given this, optimal voltage regulation in the distribution system (DS) can benefit the DS operator by reducing the costs of purchasing electric power through enforcing conservation voltage reduction (CVR) or even increasing its profit from the power sold to the customers by optimally increasing the DS voltage level. On the other hand, demand response programs (DRP) is an effective way to decrease the utility costs and increase the profit from both DS operator customers' point of view. This paper investigates the impact of incentive-based DRP and voltage regulation on the operation of DS under different objective functions. The cost of electricity consumption, the DS operator profit obtained from the electricity market, and system reliability are the three objective functions considered in this study. The reliability of DS is assessed using energy not supplied (ENS) index. The optimization problem is solved using exchange market algorithm (EMA). The optimization results are verified on the IEEE standard 33-bus test system.**

***Index Terms*—Conservation voltage reduction, demand response program, reliability, voltage regulation.**

I. Introduction

DISTRIBUTION systems (DSs) operation is rapidly evolving due to the ever-increasing communication and control technologies and integration of distributed energy resources (DERs). An advanced distribution management system (ADMS) has been proposed as a promising solution to tackle the DS challenges by integrating the conventional distribution management system and outage management system. ADMS has different tasks which among them voltage regulation (VR) and demand response program (DRP) are of particular importance [1]. ADMS can effectively improve the DS efficiency and reliability and act as a control and decision support for the DS operators (DSO) which play an important role in the power markets of future restructured power systems [2].

Tohid Khalili and Ali Bidram are supported by the National Science Foundation EPSCoR Program under Award #OIA-1757207.
Tohid Khalili and Ali Bidram are with the department of Electrical and Computer Engineering, University of New Mexico, Albuquerque, USA (e-mails: {khalili, bidram}@unm.edu).
Amirreza Jafari, Seyed Mohammad Sajjadi Kalajahi, and Behnam Mohammadi-Ivatloo are with Faculty of Electrical and Computer Engineering, University of Tabriz, Tabriz, Iran. e-mails: (jafariamirreza4@gmail.com, Mohammad.sajjadi9452@gmail.com, mohammadi@ieee.org)

VR in the distribution systems (DSs) is of particular importance to ensure that the voltage profile of DS remains in an allowable range determined by utility regulations. VR, based on the conditions and demand of the network, can be performed in the form of (i) conservative voltage reduction (CVR) which is accompanied by a reduction in the voltage level of the system, or (ii) by increasing the voltage level of DS within a permissible range. CVR has gained much attention to increase the economical profit and decrease the costs associated with the operation of power systems. CVR changes the voltage profile of distribution systems to tune up the system demand and maximize the overall profit of DSO [3, 4]. In [5], a survey on the applications of the CVR is conducted which highlights its capabilities. CVR has been used as a practical approach for peak shaving, power loss reduction, energy saving, reducing operational costs, and increasing the reliability of the power system [5]-[8]. In [6], the pros and cons of employing CVR are studied and its impacts on cost reduction and energy saving of the power system are reviewed. In [7], CVR has been considered in the optimal planning of a microgrid for optimal placement and sizing of capacitors and DERs. In [8], the effect of implementing CVR and voltage optimization on the Ireland DS is investigated from the energy-saving perspective. In [9], CVR is used to reduce peak demand and energy consumption. CVR's ability to improve the stability and reliability of the power system has been evaluated in [10]. It is shown that under emergency conditions, when there is not enough power available to supply the DS load, CVR can be applied to slightly decrease the demand. As a result, DS stability and reliability are maintained [11, 12].

VR can be combined with other techniques to achieve a multi-objective optimization in the DS. For instance, [13] proposes a novel method for simultaneous load scheduling and VR in the DS. VR and load sharing in microgrids are investigated in [14]. In [15], the optimal planning of energy storage systems and determining their optimal location and capacity by considering CVR is investigated. The objective function of this work is to minimize the total investment and operational cost by considering the energy savings resulting from CVR's implementation. In [16], the implementation of CVR in a DS is evaluated by multistage support vector regression (MSVR) based on prediction and load modeling. In [17], CVR has been implemented to reduce the power consumption of the network by using the voltage-current droop characteristic.

DRP is defined as the program that facilitates peak shaving by shifting the power consumption from one time instant to another one or load curtailment that is coordinated with customers. DRP benefits DS by decreasing its operational cost, improving its reliability, and increasing the profit gained from the sale of energy [18, 19]. Changing the pattern of energy consumption alters the system voltage profile. In [20, 21], the impact of DRP on the DS voltage is studied. In [22], emergency DRP is utilized for real-time controlling of voltage in an automated DS. Since the implementation of DRP in DS changes the network voltage level, it is worthwhile to evaluate the impact of the simultaneous implementation of incentive-based DRP and VR on the optimal operation of DS. Most of the existing research works in the literature consider the impacts of either VR or DRP on the DS. Simultaneous integration of DRP and VR has not been well investigated yet. In [1], DRP and CVR are integrated into an ADMS to increase DS efficiency and minimize the consumption cost in the day-ahead market. This reference first minimizes the load consumption with DRP and then CVR to minimize the consumption cost. Furthermore, a smart voltage optimization method is proposed in [23] to manage the industrial DRP. Besides, CVR is also implemented to reduce the loss and the demanded load in [24]. Ref. [25] presents an approach to perform the CVR for managing the loads. Additionally, the voltage of the system is utilized to improve the energy productivity and efficiency of the power system in [26, 27]

This paper further extends the proposed integrated DRP and CVR in [1] by considering a more comprehensive approach to account for the DS voltage regulation and DRP for improving the system efficiency and reliability while maximizing the profits of DS in a day-ahead power market. Our proposed approach for optimizing the network voltage is comprised of two stages, namely, the CVR implementation process and the controlled increase of system voltage level. Depending on the system condition, at each hour, one of the two mentioned stages is adopted. The voltage level is changed by adjusting the tap of load tap changer (LTC) at the distribution circuit substation transformer. The objectives for combined DRP and VR problem include the total cost of the network, the DS profit from the purchase and sale of power, and network reliability. The voltage deviation index (VDI) and $\overline{CVR}$'s (i.e., the percentage of voltage reduction caused by voltage optimization) variations due to the implementation of DRP are also investigated. The proposed methodology is implemented on the IEEE 33-bus test system, and the results are compared and analyzed with the base state of the test system. To solve the optimization problem in each of the scenarios, the exchange market algorithm (EMA) [28] is utilized. EMA is an efficient and practical algorithm in which its effectiveness is verified in several published papers [29, 30].

This paper makes the following contributions which to the best of authors' knowledge have not been exploited yet:

- The impact of optimizing the voltage level of DS over 24 hours on the DS's cost of purchased power and profit from energy sales and power loss is also evaluated by EMA.
- Simultaneous implementation of incentive-based DRP and VR on the performance of the distribution system is studied.
- The paper's VR scheme not only includes CVR but also considers the impact of intentional voltage increase on the performance of DS.
- ZIP model is used to model the customers' demand changes.

The remainder of this paper is organized as follows. In Section II, the preliminaries of the load model, incentive-based DRP, and EMA are provided. Problem formulation including the objective functions and constraints are elucidated in Section III. In Section IV, the proposed approach for CVR and optimization algorithm is described. The results of simulation and analysis are presented in Section V. Finally, Section VI concludes the paper.

II. Preliminaries

A. Voltage-Dependent Load Model

To consider the effect of voltage changes on the DS's load, the ZIP load model is utilized [31]-[33]. The ZIP model that accounts for the load active and reactive power changes caused by the voltage variations as

$$P_{i,t} = P_{i,t}^{0}\left(c_{z_p}\left(\frac{V_{i,t}}{V_{i,t}^{0}}\right)^{2} + c_{i_p}\left(\frac{V_{i,t}}{V_{i,t}^{0}}\right) + c_{p_p}\right), \qquad \forall i,t\,, \tag{1}$$

$$Q_{i,t} = Q_{i,t}^{0}\left(c_{z_q}\left(\frac{V_{i,t}}{V_{i,t}^{0}}\right)^{2} + c_{i_q}\left(\frac{V_{i,t}}{V_{i,t}^{0}}\right) + c_{p_q}\right), \qquad \forall i,t\,, \tag{2}$$

where $P_{i,t}^{0}$, $Q_{i,t}^{0}$, and $V_{i,t}^{0}$ are the active, reactive power, and voltage of bus i before voltage adjustments at time t, respectively. $P_{i,t}$, $Q_{i,t}$, and $V_{i,t}$ are the active, reactive power, and voltage of bus i after voltage adjustments at time t, respectively. c_{i_p}, c_{p_p}, c_{z_q}, c_{i_q}, c_{z_p}, and c_{p_q} are the constant coefficients of active and reactive power ZIP equations. The ZIP model can effectively incorporate the load dependency on voltage during power flow calculations. To this end, as the bus voltages are updated in each iteration of the power flow, the new values of the network loads are calculated according to (1) and (2) using the previous iteration voltage values. In this paper, the Backward-Forward power flow method is deployed [34].

B. Incentive-Based DRP Model

The incentive-based DRP can improve the reliability of DS and reduce the cost of purchased power which in turn increases the profit from the trade of energy. By considering some incentives for the customers, the incentive-based DRP reduces the consumption during peak hours by shifting power demand from peak hours to off-peak hours. An optimal DRP tends to relieve the congestion on DS while maximizing the economic benefits of customers. The multi-period incentive-based DRP model for the loads connected to the DS buses at different hours of the day can be expressed as [35]

$$P_{i,t} = P'_{i,t} \times \left[1 + E_i(t)\frac{A_t}{\rho_t} + \sum_{\substack{h=1 \\ h \neq t}}^{24} E_i(t,h)\frac{A_t}{\rho_t} \right], \tag{3}$$

where $P'_{i,t}$ and $P_{i,t}$ describe the demand of bus *i* at time *t* before and after the implementation of DRP, respectively. The self-elasticity of bus *i* at time *t* is shown by $E_i(t)$ and the cross elasticity of the bus *i* according to the time *h* is shown by $E_i(t,h)$. The cross elasticity represents the effects of paying the incentive rates at the other hours on the demand of the current hour. A_t and ρ_t show the incentive rate and electricity price at time *t*. The incentive rate and the electricity price are assumed to be constant.

C. VR

VR in a DS can be performed through LTC, voltage regulators, switched capacitors, or dynamic VAr compensators. Without loss of generality, in this paper, it is assumed that VR of DS is done by adjusting the LTC connected to the primary bus. This adjustment is carried out in a way that the voltage of all buses remains in the allowable voltage range determined by the utility regulations. VR, based on the conditions and demand of the network, can be performed in the form of a CVR which will be accompanied by a reduction in the voltage level of the system, or by increasing the voltage level within the permissible range.

D. EMA

In this paper, the proposed optimization problem is solved using EMA. According to [28, 36], optimization speed, search zone selectivity, wide optimization range, and high performance in finding the global optimum are some of the salient features of EMA. The performance of EMA versus some other conventional algorithms is compared in [28, 36]. EMA is inspired by the stock market in which stockholders can make different decisions based on rules as well as their own experience [28, 36]. In EMA, the optimization is performed in two stages corresponding to the balanced and oscillatory condition of the market. In the balanced condition of the market, stockholders can gain the highest possible profit by predicting the current situation without accounting for the risk in their transactions. However, in the oscillatory condition, stockholders intelligently exchange their stocks by taking risks to achieve a higher rank in the market. The diverse nature of the market's prevailing situations creates market complexity and different behaviors of stockholders. A successful stockholder follows other successful stockholders, utilizes experience to improve current performance, learns from the mistakes to modify the process, avoids investing in sectors that do not comply with stockholder's policy, conducts the maximum purchase in favorable conditions, does not participate in unfavorable conditions, and maintains capital in all market conditions. In EMA, each answer to the problem resembles a stockholder; optimization problem parameters resemble the stocks; each iteration of optimization is similar to a market exchange stage; in each iteration, the algorithm ranks stockholders in terms of the total value of their shares in the market [28, 36].

III. Problem Formulation

A. Objective Functions

The objective functions include cost, profit, and network reliability. The *first objective function* addresses the operational cost of the network and is comprised of the cost of purchasing power from the wholesale market and the cost of implementing the incentive-based DRP. The cost function of the distribution system is described as

$$Cost = Cost_{DR} + Cost_E , \tag{4}$$

where

$$Cost_E = \sum_{t=1}^{24} \left(P_t - ENS_t \right) \times \lambda_t , \tag{5}$$

$$Cost_{DR} = \sum_{t=1}^{24} P_{D,t} \times A_t . \tag{6}$$

Equations (5) and (6) indicate the cost of purchasing power from the wholesale market and the cost of implementing DRP. In (5), P_t and ENS_t represent the total demand and the energy not supplied (ENS) at time *t*, respectively. ENS is defined as the portion of the required energy of the customers which cannot be supplied by DS. ENS is nonzero when the DS total demand is larger than DS's maximum allowable power flow. The maximum allowable power flow is determined based on the rating of DS's substation transformer and its main branch supplying the DS's customers. λ_t specifies the cost of purchasing power from the upstream grid, and $P_{D,t}$ represents the sum of the reduced power of all customers at time t. $P_{D,t}$ is calculated by

$$P_{D,t} = \frac{1}{2} \times \sum_{i=1}^{N_b} \left| P_{DRP,i,t} \right| , \tag{7}$$

where N_b denotes the total number of buses in the system; $P_{DRP,i,t}$ denotes the amount of power of bus *i* at time *t* that is participated in DRP. It should be noted that with DRP the summation of the total daily amount of the reduced and increased power of customers should be equal to zero. Therefore, as shown in (7), half of the daily participated power in DRP is equal to the total decreased power of the customers.

The *second objective function* is the profit of DS which is defined as the difference between the revenue of selling energy to the customers and daily operational costs. This objective function is formulated as

$$Profit = \sum_{t=1}^{24} \sum_{i=1}^{N_b} P_{i,t}\rho_t - Cost_{DR} - Cost_E , \tag{8}$$

where ρ_t shows the electricity price of energy sold to customers at time *t*; $P_{i,t}$ describes the demand of bus *i* at time *t*. If DRP is implemented at bus *i*, $P_{i,t}$ is calculated using (3).

Reliability is one of the main factors for assessing the DS's power quality and customers' satisfaction. In this paper, the power flow constraints of the distribution circuit are considered as the factors impacting the reliability. These constraints are the main root causes of ENS. The DS's loading level can increase until the power flow constraints of DS's branches for supplying the peak load are violated. The ENS of a day is defined as the *third objective function* as

$$ENS = \sum_{t\in N_t} ENS_t = \sum_{t=1}^{24}\left(P_t - \left(\sum_{i=1}^{N_b}\left(P_{i,t} + P_{DRP,i,t}\right) + P_{loss,t}\right)\right), \tag{9}$$

where N_t is the sum of the hours in which the demand is greater than circuit capacity; $P_{loss,t}$ indicates the active power loss at time t, which is determined by the network's power flow; ENS_t and ENS represent the ENS at time t and the total ENS in the distribution system, respectively.

B. Constraints

The constraints include security, power flow, and DRP constraints. The network's voltage limitation and the lines' capacity are security constraints considered in the optimization problem which are defined as

$$V_{\min} \le V_{i,t} \le V_{\max}, \quad \forall t,i, \tag{10}$$

$$\sqrt{\left(Q_b^t\right)^2 + \left(P_b^t\right)^2} < S_{b,\max}, \quad b=1,2,\dots,M, \tag{11}$$

where $V_{\min}$ and $V_{\max}$ are the minimum and the maximum allowable values of the distribution system's voltage, respectively. Also, P_b^t and Q_b^t are the active and reactive power transmitted through branch b at hour t; $S_{b,\max}$ denotes the maximum apparent power allowed to transmit through branch b; M indicates the number of the branches. The other operational constraint is the power flow constraint of distribution circuit, defined as

$$S_{cir,t} \le CAP_{cir}, \quad \forall t,i, \tag{12}$$

where $S_{cir,t}$ and CAP_{cir} represent the apparent power transmitted through the main branch of the circuit at time t and the power flow constraint of the circuit, respectively.

The execution of the incentive-based DRP in the distribution system should be subject to specific constraints. Constraints considered for the DRP implementation include maximum participated power and capacity, and the incremental and decremental power balance, which are defined as

$$\left|P_{DRP,i,t}\right| < \left|0.25 \times P'_{i,t}\right|, \quad \forall t,i, \tag{13}$$

$$\sum_{t=1}^{24} \frac{\left|P_{DRP,i,t}\right|}{2} \le C_{drp}^{\max}, \quad \forall i = 1, 2, \dots, N_b, \tag{14}$$

$$\sum_{t=1}^{24} P_{DRP,i,t} = 0, \quad \forall i. \tag{15}$$

Equation (13) shows that the load's participated power per hour should be less than 25% of its maximum. Equation (14) also indicates that the sum of decremental or incremental participated power must be smaller than a certain limit. Finally, the equality of the total sum of the incremental power with the sum of decremental powers during a day is expressed in (15). Moreover, $C_{drp}^{\max}$ represents the allowable maximum participated capacity of each load in DRP.s

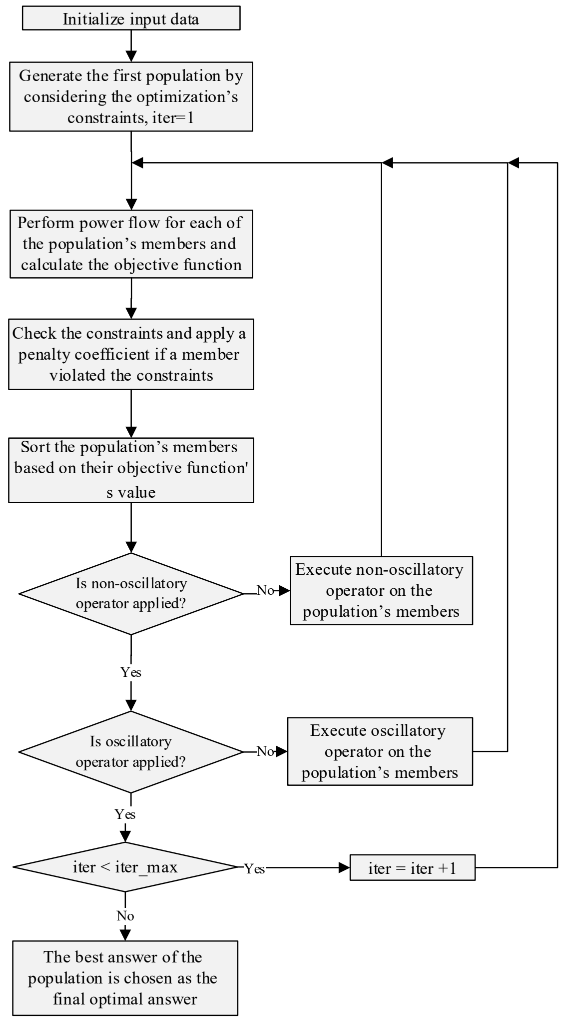

Fig.1. Flowchart of the proposed method for the CVR and the DRP.

Fulfilling the active power balance in the DS is one of the necessary constraints for power flow calculations, which is considered in the proposed optimization problem in the form of

$$P_t - ENS_t = \sum_{i=1}^{N_b}\left(P_{i,t} + P_{DRP,i,t}\right) + P_{loss,t}, \quad \forall t. \tag{16}$$

According to (16), the aggregation of the total demand of the consumers affected by the DRP and the active power loss should be equal to the supplied power considering the ENS.

IV. Methodology

The goal of this paper is to optimize the costs, profit, and reliability of DS by adjusting the voltage and executing the DRP. The proposed optimization problem is run in a day-ahead manner after the day-ahead market prices for the next day are available from the wholesale market. Even though for VR, the optimization of different hours of the day is independent, DRP's participated power at different hours highly depend on each other (see (3)). Therefore, in the proposed approach, all hours of the day should be considered in a single optimization problem. The flowchart of the proposed optimization algorithm using the EMA is shown in Fig. 1. The steps of the proposed algorithm are as follows:

Step 1. Initializing input data of the optimization problem:

In this step, the initial information including next day's hourly active and reactive power profiles, hourly day-ahead market prices, electricity price to be sold to the customers, customer incentive rates, self and cross elasticity of the network loads, circuit power flow constraint, and ZIP coefficients are initialized.

Step 2. Generating the initial population:

A population member consists of the desired optimization variables including the primary bus voltage and the participated power of each network's load in the DRP within 24 hours. The initial population including a number of members is generated considering the problem constraints. After the initial population is formed, the algorithm's iteration counter is set to one.

Step 3. Power flow and cost function calculation

In this step, for each member of the population, the power flow is performed according to the power balance and the maximum permissible power transmitted through the circuit. The power flow considers the bus voltage variations and the load demand changes according to the ZIP model. After performing the power flow, based on the results obtained, the intended objective function is calculated for all members of the population.

Step 4. Assessing the security constraints

After power flow is conducted, based on the values obtained for the bus voltages and the power of the branches, the security constraints are examined. If the security constraints are not met, a penalty factor is applied to the intended objective function which is defined as

$$FC_{j,1} = FC_{j,0} \times pen, \quad \forall j, \tag{17}$$

where *pen* represents the penalty factor for the optimization problem. $FC_{j,0}$ and $FC_{j,1}$ are the corresponding values of the j^{th} objective function before and after applying the penalty factor, respectively. *pen* is chosen large enough such that a member of the population that does not comply with the security rules loses its rank in the market and is removed from the population in the subsequent iterations.

Step 5. Sorting the population's members

In this step, population members are sorted in ascending order according to the value of their objective function, and the iteration counter of the algorithm increases by one unit.

Step 6. Applying the non-oscillatory operator

The non-oscillatory operator tackles the optimization problem assuming the balanced stock market condition as explained in Section II.D. Herein, each population member resembles a stockholder in the stock market. In the balanced stock market condition, participants exchange their stock by predicting the market condition while not taking any risks in their trades. In this case, optimization problem participants are classified into top, medium, and low rank categories. Members in top rank category seek to maintain their position in the population members' list and do not change their values. However, members in medium and low rank categories update their values using

$$pop_n^{g(2)} = r \times pop_{1,m}^{g(1)} + (1-r) \times pop_{2,m}^{g(1)}, \quad \text{with } m = 1,2,3,\cdots n_m \text{ and } n = 1,2,3,\cdots n_n, \tag{18}$$

$$pop_f^{g(3),new} = pop_f^{g(3)} + 1.6 r_1 \left(pop_{m,1}^{g(1)} - pop_f^{g(3)} \right) + 1.6 r_2 \left(pop_{m,2}^{g(1)} - pop_f^{g(3)} \right), \tag{19}$$

where $pop_{1,m}^{g(1)}$ and $pop_{2,m}^{g(1)}$ are the values of two population members selected from the top rank stockholders. $pop_n^{g(2)}$ and $pop_f^{g(3)}$ are the values of the intended member of the medium and low rank categories, respectively. n_m and n_n are the number of members in the top rank and medium rank categories, respectively. r, r_1, and r_2 are random variables between zero and one. As seen, the medium and low rank category members select their values as the average of the values of the two members selected from the top rank category.

The non-oscillatory operator changes the value of the variables. Therefore, there might be a chance that the new variable values do not comply with the problem constraints. Therefore, it is necessary to check the constraints related to the variables and make the required changes if the constraints are not satisfied. The new variable values created by the non-oscillatory operator should go through steps 3, 4, and 5 to update and sort the population's members and prepare them for the oscillatory operator.

Step 7. Applying the oscillatory operator:

In the oscillatory operating mode, market conditions are unpredictable. Therefore, stockholders carry out their exchanges considering risks. As they reduce their rankings in the market, their associated risks increase accordingly. Similar to the non-oscillatory operator, the population members are divided into three categories of top, medium, and low rank categories. Top rank category members do not change their shares to maintain their ranking in the market. However, medium rank category members update their values as

$$\Delta n_{t2} = n_{t2} - \delta + \left(2 \times r \times \mu \times \eta_2 \right), \tag{20}$$

$$\mu = \frac{t_{pop}}{n_{pop}}, \tag{21}$$

$$\eta_2 = n_{t2} \times g_2, \tag{22}$$

$$g_2^k = g_{2,\max} - \frac{g_{2,\max} - g_{2,\min}}{iter_{\max}} \times k. \tag{23}$$

In (21), Δn_{t2} represents the amount of change in the value of a variable in a member from the medium rank category. n_{t2} is the value of the intended member's variable before the oscillatory operator takes action. δ, μ, η_2 and r represent market characteristic, the rank coefficient of the intended member, risk level for the members of the second category, and a random number between zero and one, respectively. In (21), t_{pop} and n_{pop} indicate the rank of the member and the total number of population members, respectively. g_2^k and k are the risk level of the intended member from the medium rank category and the value of the algorithm's iteration counter. The low rank category members update their values as

$$\Delta n_{t3} = 4 \times r_s \times \mu \times \eta_3 , \tag{24}$$

$$r_s = 0.5 - rand , \tag{25}$$

$$\eta_3 = n_{t3} \times g_3 , \tag{26}$$

where Δn_{t3} is the amount of change in the value a variable in a member from the low rank category. n_{t3} is the value of the intended member's variable before the oscillatory operator takes action. η_3 and g_3 are the risk level of the intended member and the risk taken in the low rank category, respectively. r_s is a random number from $[-0.5,\ 0.5]$ range. *rand* denotes a uniformly distributed random number. The new variable values created by the oscillatory operator should go through steps 3, 4, and 5 to update and sort the population's members.

Step 8. Checking the algorithm termination criterion

In this step, the algorithm's iteration counter value is evaluated. If it reaches its final value, the algorithm ends, otherwise, the algorithm returns to step six.

Step 9. Selecting the final optimal solution

In the last step, the member with the best ranking in population, which has the optimal value of the objective function, is chosen as the final optimal answer to the problem.

V. Results and Discussion

To verify the effectiveness of the proposed optimization problem and evaluate the impact of DRP and VR on the presented objective functions, first, DRP and VR are implemented individually, and then, they are integrated. To study the impact of implementing VR and the incentive-based DRP on the discussed objective functions, eight different scenarios are considered as listed in Table I. Scenario 1 is considered as a baseline when the circuit power flow is not constrained. On the other hand, Scenario 6 denotes a baseline scenario assuming that the circuit has a power flow constraint. In these two scenarios, no optimization is performed. However, the objective functions are calculated to facilitate the comparison of results gathered form optimization scenarios with the baseline scenarios. In Scenarios 2 and 3, the VR is performed considering the cost and profit of the network as the objective functions, respectively. Scenarios 4 and 5 simultaneously apply CVR and DRP considering the cost and profit of the network as the objective functions, respectively. As seen, Scenarios 1 to 5 do not consider the circuit capacity constraint, while this constraint is involved in the optimization process for Scenarios 6 to 8.

Simulations are conducted in MATLAB using the IEEE 33-bus distribution system [37], shown in Fig. 2. The cost of energy sales is considered to be at a constant rate of 3.5 ¢/kWh and the hourly price of electricity in the market is shown in Fig. 3 [3]. The incentive rate paid in the DRP is 1 ¢/kWh. The power flow constraint of the circuit is considered to be 4 MVA. The values of the self and cross elasticity used in the DRP are shown in Table II [38]. In this work, a load below 2.8 MW is considered as an off-peak load, between 2.8 and 3.3 MW is considered as a partial-peak average load, and above 3.3 MW is considered as a peak load. Additionally, the values of $V_{\min}$ and $V_{\max}$ are set to 0.9 and 1.05, respectively. It is assumed that LTC can change the DS voltage using 32 consecutive taps. The coefficients of the ZIP model of the residential customers are presented in Table III [39]. The maximum participation capacity involved in the DRP is 8 MW.

A. VR and DRP Impacts in Scenarios 1 to 5

Table IV shows the amount of energy purchased, sold, and lost in Scenarios 1 to 5. As mentioned, Scenario 1 is considered as the baseline. In Scenario 2, since the objective function is to minimize the cost of purchasing energy from the main grid by implementing VR, primary bus voltage reaches its minimum allowable value which in turn reduces the amount of energy purchased. Therefore, it is observed that the amount of energy purchased and, consequently, the energy sold in Scenario 2 is less than the baseline Scenario 1. In Scenario 4, by integrating incentive-based DRP to CVR, the amount of purchased and sold energy, and the power loss of the system are decreased compared to Scenario 2. The reason is that DRP smooths out the daily load profile. This results in a relatively higher voltage profile of the circuit, which in turn increases the flexibility of utilizing LTC tap and further voltage reduction through CVR.

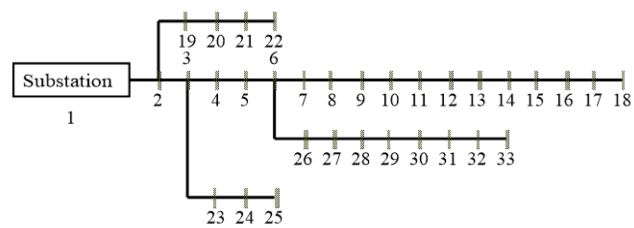

Fig. 2. IEEE 33-bus system single line diagram.

TABLE I
Test Scenarios and Corresponding Objective Functions

Number	Scenario	Objective Function
1	Base case	-
2	Considering VR	Cost
3	Considering VR	Profit
4	Considering VR and DRP	Cost
5	Considering VR and DRP	Profit
6	Considering circuit power flow constraint	-
7	Considering circuit capacity limitation and VR	ENS
8	Considering circuit capacity limitation, VR, and DRP	ENS

TABLE II
Self and Cross Elasticity of the 33-bus Network Loads

#	Peak load	Partial-peak load	Off-peak load
Peak load	-0.1	0.16	0.12
Mean load	0.16	-0.1	0.1
Off-peak load	0.12	0.1	-0.1

TABLE III
Coefficients Of Zip Model

Class of Customers	c_{z_p}	c_{i_p}	c_{p_p}	c_{z_q}	c_{i_q}	c_{p_q}
Residential	0.85	-1.12	1.27	10.96	-18.73	8.77

TABLE IV
PURCHASED, SOLD, AND LOST ENERGY [MWH] IN SCENARIOS 1-5

Scenario	Purchased energy	Sold energy	Lost energy
SC_1	78.2854	75.7857	2.4997
SC_2	76.5460	73.9145	2.6315
SC_3	80.0629	77.6255	2.4374
SC_4	75.7020	73.1758	2.5262
SC_5	80.1220	77.6654	2.4566

TABLE V
DEMAND COST, LOSS COST, DRP COST, TOTAL COST, REVENUE, AND PROFIT [$] IN SCENARIOS 1TO 5

Scenario	DC	LC	DRPC	TC	Revenue	Profit
SC_1	2448.1	81.1	0	2529.3	2652.5	123.1
SC_2	2388.0	85.4	0	2473.4	2587.0	113.5
SC_3	2505.5	79.2	0	2584.7	2716.8	132.1
SC_4	2362.8	81.9	12.05	2456.7	2561.2	104.4
SC_5	2491.9	83.3	8.51	2579.2	2718.3	139.1

It should be noted that DRP only shifts a portion of the load from one hour to another and does not affect the total load. Since the objective function of Scenario 3 is the profit from the sale of energy, the voltage profile is slightly increased in the hours with low electricity price to increase the amount of purchased energy. As seen in Table IV, the implementation of the DRP and VR in Scenario 5 increases the amount of purchased and sold energy. However, if one compares the results of Scenario 5 and 3 versus the results of Scenario 4 and 2, Scenario 5 is less effective than Scenario 4. Therefore, one can conclude that the implementation of the DRP and CVR with cost as the objective is more effective than DRP and voltage increase with profit as the objective.

In Table V, the calculated demand cost (DC), loss cost (LC), DRP cost (DRPC), total cost (TC), revenue, and profit are listed. Table V shows that TC decrease in Scenario 4 compared to Scenario 2 and profit increase in Scenario 5 compared to Scenario 3 due to the implementation of incentive-based DRP. The reason is that in Scenario 4, the DRP transfers loads from hours with high electricity price to low price hours to reduce the cost of purchasing energy throughout the day. In Scenario 5, DRP increases the profit of selling energy by transferring the load to hours that purchase price is lower than the sale price. Fig. 3 shows the 24-hour load profile of the network along with the hourly electricity price in the market for Scenarios 1 to 3. As seen, in Scenario 2, the CVR reduces the network's load profile compared to the network's base mode during all hours of the day. In Scenario 3, when the energy price in the market is lower than the cost of selling energy (3.5 ¢/kWh), the voltage level is slightly stepped up to increase the loading level and achieve a higher profit. Additionally, when the market price is higher than the sales price in the network, the load profile decreases by decreasing the network voltage within the allowable voltage range.

B. VR and DRP Impacts in Scenarios 6 to 8

Table VI shows the amount of energy purchased, sold, and lost in Scenarios 6 to 8. In these scenarios, the circuit power flow constraint is considered and ENS is the objective function. In Scenario 7, the amount of purchased and sold energy is reduced compared to Scenario 1, and since the objective function is minimizing the ENS, by employing VR, the amount of energy bought and sold increases compared to Scenario 6 to improve the reliability. In Scenario 8, although the implementation of the DRP does not directly affect the total energy consumption, it improves the VR performance and increases the energy purchased from the wholesale market and the energy sold to the customers as well.

Table VII represents the TC, profit, DRPC, and ENS for Scenarios 6 to 8. Simulation results show that VR reduces the ENS. CVR decreases the voltage level of the network and, consequently, the overall loading of the network, which in turn reduces the ENS. The combined VR and DRP reduces ENS more than the sole implementation of VR. However, this is achieved at the cost of reducing profit as seen in Scenario 8. The DRP transmits the load from peak hours to off-peak hours and by solving the circuit power flow constraints, reduces the ENS, and improves the reliability of the network.

C. Impacts of Optimization Algorithms on the Voltage of Distribution System

To show the impact of DRP and VR optimization algorithms on the voltage of the distribution system, two indices are used as seen in Table VIII. The first index is VDI, formulated as

$$VDI = \frac{\sum_{t=1}^{24}\sum_{i=1}^{33}(V_{i,t}-V_i^0)^2}{T}, \tag{27}$$

where $V_{i,t}$ denotes the voltage of bus i at time t; V_i^0 is bus i nominal voltage. T is set equal to 24. The second index is $\overline{CVR}$ of the network which represents the percentage of voltage reduction caused by voltage optimization. $\overline{CVR}$ [40] is formulated as

$$\overline{CVR} = \frac{\sum_{t=1}^{24}\sum_{i=1}^{33}(V_{i,t}^0-V_{i,t}^1)}{T\times N_b}\times 100, \tag{28}$$

where $V_{i,t}^0$ and $V_{i,t}^1$ represent the per-unit voltage of the bus i at time t before and after VR implementation, respectively.

TABLE VI
PURCHASED, SOLD, AND LOST ENERGY [MWH] IN SCENARIOS 6-8

Scenario	Purchased energy	Sold energy	Lost energy
SC_6	76.8202	74.3722	2.4480
SC_7	77.0782	74.5856	2.4926
SC_8	77.5442	75.0362	2.5080

TABLE VII
TOTAL COST, PROFIT, DRP COST [$], AND ENS VALUE [MWH] IN SCENARIOS 6 TO 8

Scenario	TC	Profit	DRPC	ENS
SC_6	2477.98	125.04	0	1.4618
SC_7	2485.24	125.60	0	0.8808
SC_8	2516.46	109.80	16.62	0.3847

TABLE VIII
VOLTAGE DEVIATION INDEX AND CVR VALUES

#	SC_1	SC_2	SC_3	SC_4	SC_5	SC_6	SC_7	SC_8
VDI	0.059	0.187	0.043	0.256	0.046	0.056	0.112	0.086
CVR	-	4.70	-5.17	5.12	-3.75	-	1.21	0.94

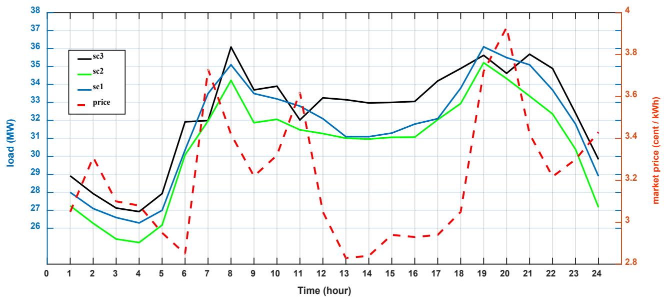

Fig. 3. Network daily load profile and the electricity price in the market.

Table VIII shows that in Scenario 2 the VDI is increased by decreasing the network's voltage level. In Scenario 3, the CVR reduces the VDI value to achieve a higher profit. In Scenario 4, with the integration of DRP and CVR, VDI is higher than Scenario 2 as a result of a further decrement in the network's voltage level. In Scenario 5, the integration of DRP and CVR results in the further increase of the network's voltage level and VDI compared to Scenario 3. In Scenario 7, by decreasing the network voltage level, the VDI value has increased compared to the baseline Scenario 6. In Scenario 8, the simultaneous execution of DRP and CVR reduces VDI compared to Scenario 7. The reason is that DRP transfers load from peak hours to off-peak hours and increases network voltage level. The positive and negative $\overline{CVR}$ index denote the increase and decrease of network voltage level compared to the normal voltage, respectively. In scenarios with the cost of energy purchasing as the objective function, the value of this index is positive. However, in the scenarios where the profit from the sale of energy is the objective function, the value of this index is negative. In scenarios with ENS as the objective function, the value of $\overline{CVR}$ is positive due to the reduction in the voltage level.

VI. Conclusion

In this paper, the impact of incentive-based DRP and VR on the operation of DSs is investigated. The considered objective functions are cost minimization, reliability improvement, and profit maximization. The cost of purchasing power from the main grid and the cost of implementing the incentive-based DRP are considered as network operational costs. The ENS index is selected to evaluate network reliability. The effective factor in reducing reliability is the limited capacity of the power transmitted through the circuit. EMA is used to solve the optimization problem. The ZIP coefficient model is used to model the load's dependence on the voltage. $\overline{CVR}$ and VDI indices are utilized and calculated to highlight the impact of optimization algorithms on the distribution system voltage.

The proposed approach is verified on IEEE 33 bus test system. Simulation results indicate that the integration of DRP and VR can improve the DS reliability while increasing the profit of DS. The implementation of the CVR in the network decreases the cost of the purchased energy by decreasing the voltage level. Moreover, increasing the voltage level when the price of electricity in the market is lower than the price of the network increases the profit from selling energy. By reducing the network load as a result of reducing the voltage level, the ENS is minimized and the network's reliability is improved. Although the incentive-based DRP does not directly affect the amount of network demand, it improves the reliability of the network by helping with the VR.

References

[1] M. S. Hossan and B. Chowdhury, "Integrated CVR and Demand Response Framework for Advanced Distribution Management Systems," *IEEE Trans. Sustain. Energy*, vol. 11, no. 1, pp. 534–544, Jan. 2020.

[2] "Future role of distribution system operators" [Online]. Available: https://www.irena.org/-/media/Files/IRENA/Agency/Publication/2019/Feb/IRENA_Landscape_Future_DSOs_2019.PDF?la=en&hash=EDEBEDD537DE4ED1D716F4342F2D55D890EA5B9A.

[3] S. Gharebaghi and A. Safdarian, "Voltage regulation in private environment: Opportunity or threat," *IEEE Trans. Power Deliv.*, vol. 33, no. 6, pp. 3218–3219, Dec. 2018.

[4] Z. Wang and J. Wang, "Review on implementation and assessment of conservation voltage reduction," *IEEE Trans. Power Syst.*, vol. 29, no. 3, pp. 1306–1315, May. 2014.

[5] F. de León, M. Diaz-Aguiló, and A. Raza, "Conservation voltage reduction," *Smart Grid Handb.*, pp. 1–25, Aug. 2016.

[6] P. K. Sen and K. H. Lee, "Conservation voltage reduction technique: An application guideline for smarter grid," in *Rural Electric Power Conference (REPC), 2014 IEEE*, pp. B1-1, Jun. 2014.

[7] M. Gheydi, A. Nouri, and N. Ghadimi, "Planning in microgrids with conservation of voltage reduction," *IEEE Syst. J.*, vol. 12, no. 3, pp. 2782–2790, Sept. 2018.

[8] E. Diskin, T. Fallon, G. O'mahony, and C. Power, "Conservation voltage reduction and voltage optimisation on Irish distribution networks," *CIRED 2012 Workshop: Integration of Renewables into the Distribution Grid*, Lisbon, pp. 1-4, Sept. 2012.

[9] A. Faruqui, K. Arritt, and S. Sergici, "The impact of AMI-enabled conservation voltage reduction on energy consumption and peak demand," *Electr. J.*, vol. 30, no. 2, pp. 60–65, Mar. 2017.

[10] M. Castro, A. Moon, L. Elner, D. Roberts, and B. Marshall, "The value of conservation voltage reduction to electricity security of supply," *Electr. Power Syst. Res.*, vol. 142, pp. 96–111, Jan. 2017.

[11] D. Mak and D.-H. Choi, "Hierarchical Look-Ahead Conservation Voltage Reduction Framework Considering Distributed Energy Resources and Demand Reduction," *Energies*, vol. 11, no. 12, p. 3250, Nov. 2018.

[12] U. S. Selamogullari and A. Alsaad, "Analysis of a Residential Distribution System with the Application of Conservation Voltage Reduction at House Level," in *2019 1st Global Power, Energy and Communication Conference (GPECOM)*, 2019, pp. 430–434.

[13] J. Ren, J. Hu, R. Deng, D. Zhang, Y. Zhang, and X. S. Shen, "Joint load scheduling and voltage regulation in the distribution system with renewable generators," *IEEE Trans. Ind. Informatics*, vol. 14, no. 4, pp. 1564–1574, Apr. 2018.

[14] M. A. Setiawan, A. Abu-Siada, and F. Shahnia, "A new technique for simultaneous load current sharing and voltage regulation in DC microgrids," *IEEE Trans. Ind. Informatics*, vol. 14, no. 4, pp. 1403–1414, Apr. 2018.

[15] Y. Zhang, S. Ren, Z. Y. Dong, Y. Xu, K. Meng, and Y. Zheng, "Optimal placement of battery energy storage in distribution networks considering conservation voltage reduction and stochastic load composition," *IET Gener. Transm. Distrib.*, vol. 11, no. 15, pp. 3862–3870, Oct. 2017.

[16] Z. Wang, M. Begovic, and J. Wang, "Analysis of conservation voltage reduction effects based on multistage SVR and stochastic process," *IEEE Trans. Smart Grid*, vol. 5, no. 1, pp. 431–439, Jan. 2014.

[17] A. M. Pasha, H. H. Zeineldin, A. S. Al-Sumaiti, M. S. El Moursi, and E. F. El Sadaany, "Conservation voltage reduction for autonomous microgrids based on V–I droop characteristics," *IEEE Trans. Sustainable Energy*, vol. 8, no. 3, pp. 1076–1085, Jul. 2017.

[18] M. J. V. Pakdel, S. Ghaemi, B. Mohammadi-Ivatloo, J. Salehi, and P. Siano, "Modeling Non-Cooperative Game of GENCOs' Participation in Electricity Markets with Prospect Theory," *IEEE Trans. Ind. Informatics*, Feb. 2019.

[19] M. Alipour, B. Mohammadi-Ivatloo, and K. Zare, "Stochastic scheduling of renewable and CHP-based microgrids," *IEEE Trans. Ind. Informatics*, vol. 11, no. 5, pp. 1049–1058, Oct. 2015.

[20] M. Bayat, K. Sheshyekani, M. Hamzeh, and A. Rezazadeh, "Coordination of distributed energy resources and demand response for voltage and frequency support of MV microgrids," *IEEE Trans. Power Syst*, vol. 31, no. 2, pp. 1506–1516, Mar. 2016.

[21] N. Venkatesan, J. Solanki, and S. K. Solanki, "Residential demand response model and impact on voltage profile and losses of an electric distribution network," *Appl. Energy*, vol. 96, pp. 84–91, Aug. 2012.

[22] A. Zakariazadeh, O. Homaee, S. Jadid, and P. Siano, "A new approach for real time voltage control using demand response in an automated distribution system," *Appl. Energy*, vol. 117, pp. 157–166, Mar. 2014.

[23] A. Madhavan, B. Lee, C. A. Cañizares and K. Bhattacharya, "A smart voltage optimization approach for industrial load demand response," in *2019 IEEE Milan PowerTech*, Milan, Italy, 2019, pp. 1-6.

[24] A. Mahendru and R. K. Varma, "Reduction in system losses and power demand by combination of optimal power flow and conservation voltage reduction using smart PV inverters," *2019 IEEE Power & Energy Society General Meeting (PESGM)*, Atlanta, GA, USA, 2019, pp. 1-5.

[25] S. Singh, V. B. Pamshetti and S. P. Singh, "Time horizon-based model predictive volt/var optimization for smart grid enabled CVR in the presence of electric vehicle charging loads," *IEEE Trans. Ind. Appl.*, vol. 55, no. 6, pp. 5502-5513, Nov.-Dec. 2019.

[26] S. Jayaraman, M. Miranbeigi, R. P. Kandula and D. Divan, "Improving energy efficiency and productivity at industrial plants using dynamic voltage management," *IEEE Trans. Ind. Appl.*, vol. 56, no. 2, pp. 1250-1257, March-April 2020.

[27] R. Anilkumar, G. Devriese and A. K. Srivastava, "Voltage and reactive power control to maximize the energy savings in power distribution system with wind energy," *IEEE Trans. Ind. Appl.*, vol. 54, no. 1, pp. 656-664, Jan.-Feb. 2018.

[28] N. Ghorbani and E. Babaei, "Exchange market algorithm," *Appl. Soft Comput. J.*, vol. 19, pp. 177–187, Jun. 2014.

[29] T. Khalili, A. Jafari, M. Abapour, and B. Mohammdi-Ivatloo, "Optimal battery technology selection and incentive-based demand response program utilization for reliability improvement of an insular microgrid," *Energy*, vol. 169, pp. 92–104, Feb. 2019.

[30] T. Khalili, A. Jafari, and E. Babaei, "Scheduling and siting of storages considering power peak shaving and loss reduction by exchange market algorithm," in *IEEE Proceedings 2017 Smart Grid Conference, SGC 2017*, Mar. 2018.

[31] G. McLorn, J. Morrow, D. Laverty, R. Best, X. Liu, and S. McLoone, "Enhanced ZIP load modelling for the analysis of harmonic distortion under Conservation Voltage Reduction," *CIRED-Open Access Proc. J.*, vol. 2017, no. 1, pp.1094–1097, Oct. 2017.

[32] J. Zhao, Z. Wang, and J. Wang, "Robust time-varying load modeling for conservation voltage reduction assessment," *IEEE Trans. Smart Grid*, vol. 9, no. 4, pp. 3304–3312, Jul. 2018.

[33] Z. Wang and J. Wang, "Time-varying stochastic assessment of conservation voltage reduction based on load modeling," *IEEE Trans. Power Syst.*, vol. 29, no. 5, pp. 2321–2328, Sept. 2014.

[34] T. Khalili, M. T. Hagh, S. G. Zadeh, and S. Maleki, "Optimal reliable and resilient construction of dynamic self-adequate multi-microgrids under large-scale events," *IET Renew. Power Gener.*, vol. 13, no. 10, pp. 1750–1760, Jul. 2019.

[35] T. Khalili, A. Bidram, and M. J. Reno, "Impact study of demand response program on the resilience of dynamic clustered distribution systems," *IET Gener. Transm. Distrib.*, Apr. 2020.

[36] A. Jafari, T. Khalili, E. Babaei, and A. Bidram, "A Hybrid Optimization Technique Using Exchange Market and Genetic Algorithms," *IEEE Access*, vol. 8, pp. 2417–2427, 2020.

[37] R. Parasher, "Load flow analysis of radial distribution network using linear data structure," *arXiv Prepr. arXiv1403.4702*, Mar. 2014.

[38] H. A. Aalami, M. P. Moghaddam, and G. R. Yousefi, "Demand response modeling considering Interruptible/Curtailable loads and capacity market programs," *Appl. Energy*, vol. 87, pp. 243–250, Jan. 2010.

[39] M. Diaz-Aguiló, J. Sandraz, R. Macwan, F. De Leon, D. Czarkowski, C. Comack, and D. Wang, "Field-validated load model for the analysis of CVR in distribution secondary networks: Energy conservation," *IEEE Trans. Power Deliv.*, vol. 28, no. 4, pp. 2428–2436, Oct. 2013.

[40] A. Dorrody. (2014). *Evaluation of Conservation Voltage Reduction as a Tool for Demand Side Management.* [Online]. Available: https://digitalscholarship.unlv.edu/thesesdissertations/2075/